Engineering Structures 172 (2018) 285–292

Contents lists available at ScienceDirect

Engineering Structures

journal homepage: www.elsevier.com/locate/engstruct

# Motion tracking of a wind turbine blade during lifting using RTK-GPS/INS

K. Maes*, G. De Roeck, G. Lombaert

*KU Leuven, Department of Civil Engineering, Kasteelpark Arenberg 40, B-3001 Leuven, Belgium*

ARTICLE INFO

*Keywords:*
Motion tracking
GPS
Fiber optical gyroscope
Total station
Data fusion

ABSTRACT

This paper presents a case of object motion tracking where a real-time kinematic Global Positioning System (RTK-GPS) is used for correction of data obtained from an inertial navigation system (INS). The displacements obtained from the RTK-GPS and the accelerations obtained from the INS are combined using an unscented Kalman filter (UKF). The combined data are used to assess the motion of a 6 MW turbine blade during a hoisting operation and are compared to the blade motion obtained by use of three Leica total stations, that have been used for verification. Special focus in this paper goes to merging of heterogeneous data (displacements, rotations, and accelerations) obtained from different measurement systems. Analysis of the motion data shows that the RTK-GPS/INS measurement system allows for very accurate recording of displacement and rotation measurements.

## 1. Introduction

Motion tracking of large structures is a challenging problem. For structures that are subjected to small displacements, traditional structural displacement sensors can be used, such as linear variable differential transformers (LVDTs), that measure the displacement of the structure with respect to a fixed point in the environment [1]. The construction of a fixed reference point for installation of the sensor is often difficult or impossible, especially when dealing with large structures [2]. The use of a laser Doppler vibrometer (LDV) allows for a large distance between the measurement point and the sensor, as well as the surveying/scanning of a grid of measurement points on the structure [3–5]. The same holds for displacement measurements based on digital image processing [6,7], where a digital video camera is used to capture the motion of one or several points on the structure. Many studies have been performed to investigate the use of the Global Positioning System (GPS) measuring the global deformation of large structures [8–10]. The combination of real-time kinematic (RTK) with GPS allows for dynamic position measurements with a Root Mean Square (RMS) accuracy of ± 5 mm for the horizontal position and ± 10 mm for the vertical position. The RTK-GPS system has been used successfully in several case studies, including dynamic monitoring of the Humen Bridge, China [11], and the Nottingham Wilford suspension footbridge, UK [12]. The main advantage of GPS-based displacement measurement is its autonomous applicability, not requiring a fixed point in the direct environment of the structure. This is a major benefit for application on offshore or other large civil engineering structures. The main disadvantages of GPS and RTK-GPS are the limited sampling rate (up to 10 Hz) and disturbances due to structural elements in the direct environment of the measurement point. As an alternative to direct displacement measurements, displacements can also be obtained indirectly by (numerical) double integration of measured accelerations [13]. This technique is adopted in so-called inertial navigation systems (INS). As low frequency noise on the acceleration data tends to blow up in the integration, highpass filtering of the displacements is required to avoid a low frequency drift of the calculated displacements. The low frequency (and DC) components of the displacements can therefore not be retrieved from measured accelerations. GPS/INS was developed to obtain drift-free displacement and rotation measurements at a rate which can be much higher than the sampling rate of the GPS. Additionally, the GPS/INS approach has the advantage that the INS can continue with the computation of the location even when the GPS signal is lost (for a short time period). GPS/INS is commonly used for the navigation of aircrafts and ships and several automobile applications [14,15]. GPS/INS sensor fusion generally involves a nonlinear filtering problem, which is mostly solved by means of the extended Kalman filter (EKF) or the unscented Kalman filter (UKF). A comparison of both filtering approaches for GPS/INS data fusion is provided in [16].

The focus of this paper is on the fusion of RTK-GPS data with INS data to obtain highly accurate displacement measurements. The RTK-GPS/INS measurement system is used for dynamic measurements that have been carried out in order to verify the effectiveness of the recently developed Boom Lock© system under wind loading. The Boom Lock© system (Fig. 1a) is a tool developed by High Wind NV to reduce wind-

* Corresponding author.
*E-mail address:* kristof.maes@kuleuven.be (K. Maes).

https://doi.org/10.1016/j.engstruct.2018.06.041
Received 16 January 2017; Received in revised form 7 June 2018; Accepted 11 June 2018

**Fig. 1.** (a) The Boom Lock© system active during the installation of a wind turbine nacelle, (b) the jack up vessel Neptune, and (c) lifting configuration for the measurement campaign.

induced motion of the hoisted load, such as a turbine blade, during the installation by a mast crane, enabling the offshore installation of wind turbine components at large wind speeds. In order to evaluate the performance of the Boom Lock© system, a measurement campaign has been carried out after installation of the first Boom Lock© on the jack up vessel Neptune, owned by GeoSea NV (Fig. 1b). The measurement campaign has been performed in the harbor of Ostend, Belgium. In the experiments, an RTK–GPS/INS measurement system is used to record the motion of a 6 MW turbine blade during lifting (Fig. 1c). The displacements obtained from an RTK-GPS are combined with the accelerations obtained from an INS using an unscented Kalman filter (UKF). The blade motion obtained from the RTK-GPS/INS is compared to the motion obtained by three Leica total stations, that have been used for verification of the results. In addition, the vibrations of the crane boom and the Boom Lock© have been monitored using high accuracy three-dimensional acceleration recorders. Special focus in this paper is on the combined use of different measurement systems and different types of data in the analysis.

The outline of the paper is as follows. Section 2 describes the experimental procedure. Next, in Section 3, the motion of the turbine blade is studied. Section 4 concludes the paper.

## 2. Measurement setup

The measurements discussed in this paper have been performed in the harbor of Ostend, from 28 February 2015 to 2 March 2015. The measurement system was used to assess the motion of (1) a 6 MW turbine blade and (2) a dummy nacelle during a hoisting operation. Only the motion of the turbine blade is presented in the following.

The displacements of the turbine blade and its accelerations have been monitored, as well as the accelerations of the Boom Lock© and the crane boom. The displacements of the blade characterize its low frequency (rigid body) motion, whereas the accelerations characterize its high frequency motion, including deformations. For the remainder of this paper, whenever motion is mentioned, this refers to low frequency displacements, whereas the accelerations are referred to as the corresponding vibrations. The measurement setup for the turbine blade, the Boom Lock©, and the crane boom, is discussed in the following subsections.

### 2.1. Turbine blade

The motion of the turbine blade has been measured using an iXBlue HYDRINS high performance Inertial Navigation System (INS) combined with RTK-GPS. In addition, three Leica TRCP 1201 total stations are used for reference measurements. Additional acceleration measurements on the blade have been performed using four wireless GeoSIG GMS-18 recorders. Fig. 2 gives an overview of the measurement locations of the sensors installed on the turbine blade. Table 1 provides further specifications of the measurement devices. The different measurement systems are discussed next.

*iXBlue HYDRINS RTK-GPS/INS.* The iXBlue HYDRINS system (Fig. 3a) includes three fiber optic gyroscope (FOG) sensors and a three-axial accelerometer to measure its three-dimensional motion. The position (3 translations, 3 rotations) of the sensor is obtained by integration of the measured acceleration and FOG data (sampling rate 50 Hz) using an unscented Kalman filter. Additional position measurements obtained from an MGB-Tech RTK-GPS with Septentrio AsteRx2eL GNSS board (sampling rate 5 Hz) are accounted for in the integration process in order to correct inaccurate low-frequency results obtained by the integration. The data fusion is performed using the software package DELPH INS [17], provided by iXBlue, yielding the motion of the blade at a sampling rate of 50 Hz. The data processing starts from the measured acceleration, FOG, and RTK-GPS data, that received a time stamp from the GPS as to secure time synchronization. The filtering procedure adopted by DELPH INS is described in [18] and briefly summarized hereafter. The reader is referred to [19,20] for more details on the UKF algorithm.

The translations and rotations of the HYDRINS sensor are estimated from the measured acceleration and FOG data as would be the case for a regular INS. This process is performed at a rate of 50 Hz. Each time additional data from the RTK/GPS becomes available, i.e. every 0.2 s, it is compared to the estimates provided by the INS by means of the UKF. This comparison is then used to update an error model for both the INS sensors (accelerometers and FOGs) and the RTK-GPS. These error models account for both measurement noise and sensor bias. Finally, adopting these error models to weigh the INS and RTK-GPS data results in corrected translation and rotation estimates. The INS uses these estimates as starting point for the estimation in the next 0.2 s.

The combination of the INS with RTK-GPS allows for dynamic position measurements with an RMS error of about 1 mm for the horizontal position and 2 mm for the vertical position. The rotations (heading, roll, and pitch) are obtained with an accuracy of about 0.01° RMS. The RTK-GPS/INS system does not require a fixed reference point in the direct environment of the structure and is therefore particularly well suited for offshore applications.

The HYDRINS system and RTK-GPS have been installed near the root of the blade, i.e. where the blade is to be connected to the rotor. The HYDRINS system was put inside a box, that is mounted on top of the blade using fixation belts (see Fig. 4). The RTK-GPS was mounted on top of this box. The HYDRINS system is aligned with the global coordinate system *xyz*, that has its origin at the center of gravity (COG) of the blade (see Fig. 2).

*Leica TRCP 1201 total stations.* The three Leica TRCP 1201 total stations (Fig. 3b) allow continuous tracking of one prism each, combining accurate angle and distance measurements to obtain an estimate of the location of the prisms in three dimensions. The position measurements have an accuracy of ± 3 mm RMS. Leica 360 YR20A prisms (Fig. 3c) are attached to the turbine blade at three different locations. The locations are determined such that the rigid body motion of the blade can be reconstructed from the measured motion of the prisms (Figs. 2 and 4). The total stations are installed on the quay wall of the

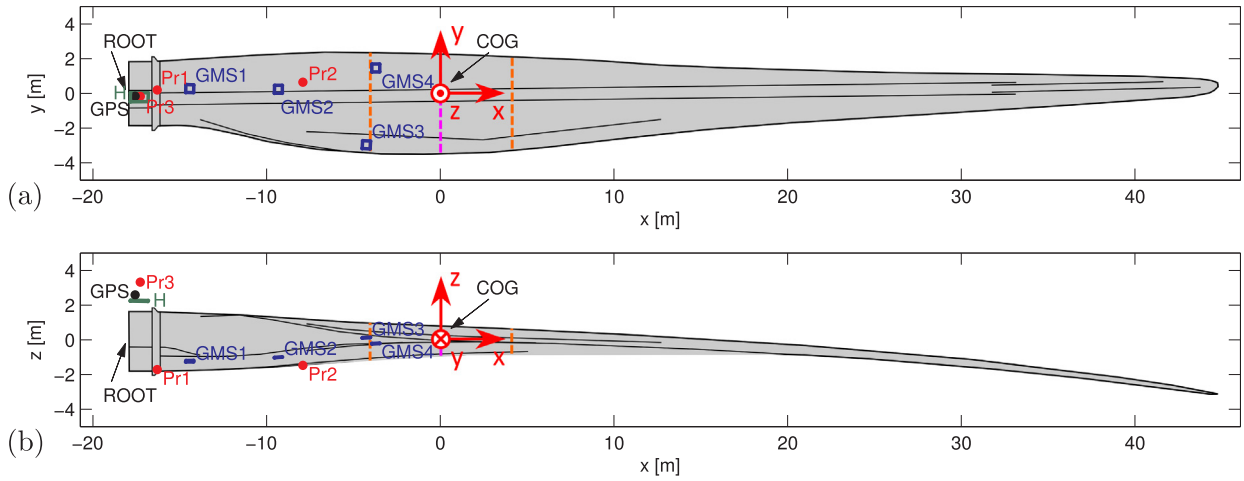


**Fig. 2.** (a) Top view and (b) side view of the turbine blade indicating the sensor positions (`H`: HYDRINS RTK-GPS/INS, `Pri`: prism *i*, and `GMSi`: GeoSIG GMS-18 unit *i*). For the HYDRINS and the GeoSIG GMS-18 sensors, the corners of the cabinet containing the sensors are shown. The blade gripper supports are indicated by a dashed orange line. The coordinate system *xyz* has its origin at the COG of the blade. (For interpretation of the references to color in this figure legend, the reader is referred to the web version of this article.)

**Table 1**
Overview of the different measurement devices adopted in the measurement campaign.

| Measurement device | Measurement type | Units | RMS error |
|---|---|---|---|
| iXBlue HYDRINS | | | |
| – Fiber optic gyroscopes | Angular velocity | [°/s] | 0.001°/s |
| – Three-axial accelerometer | Acceleration | [m/s$^2$] | 0.01 m/s$^2$ |
| MGB-Tech RTK-GPS | | | |
| – RTK-GPS | Horizontal position X | [m] | 0.006 m* |
| | Horizontal position Y | [m] | 0.006 m* |
| | Altitude | [m] | 0.01 m* |
| * Measurement accuracy corresponding to a sampling rate of 1 Hz. | | | |
| GeoSIG GMS-18 | | | |
| – Three-axial accelerometer | Acceleration | [m/s$^2$] | 1.2 × 10$^{-4}$ m/s$^2$ |
| Leica TRCP 1201 total station | | | |
| – 3D Position measurement | Horizontal position X | [m] | 0.003 m |
| | Horizontal position Y | [m] | 0.003 m |
| | Altitude | [m] | 0.003 m |
| iXBlue OCTANS 3000 | | | |
| – Fiber optic gyroscopes | Angular velocity | [°/s] | 0.001 °/s |
| – Three-axial accelerometer | Acceleration | [m/s$^2$] | 0.01 m/s$^2$ |

harbor. The need for a fixed reference point in the direct environment of the structure impedes the use of total stations for offshore applications. In addition, whenever the line of sight of a total station is interrupted, e.g. by the crane boom when a slewing operation is performed (see Fig. 5), the motion tracking is disturbed. In this case, the location of the total station on the quay wall is changed in order to avoid interruption.

The total stations log the prism coordinates at a rate of about 1 sample per second (i.e. 1 Hz). Since the rate is variable, the logging data are interpolated to a common time base. The data are synchronized manually with the GPS-timestamped data obtained from the other sensors (HYDRINS, OCTANS 3000 and GMS-18 units), by correlating the altitude (vertical position of the blade) measured by the Leica total stations and the HYDRINS system.


**Fig. 4.** Overview of the HYDRINS and prisms installed on the turbine blade.

*GeoSIG GMS-18.* The GeoSIG GMS-18 recorders (Fig. 3d) are used to measure the vibrations of the blade in addition to the motion measured by the RTK-GPS/INS system and the total stations. The GeoSIG GMS-18 recorders include a three-axial accelerometer for high accuracy vibration monitoring. Each recorder has its own data acquisition system. A

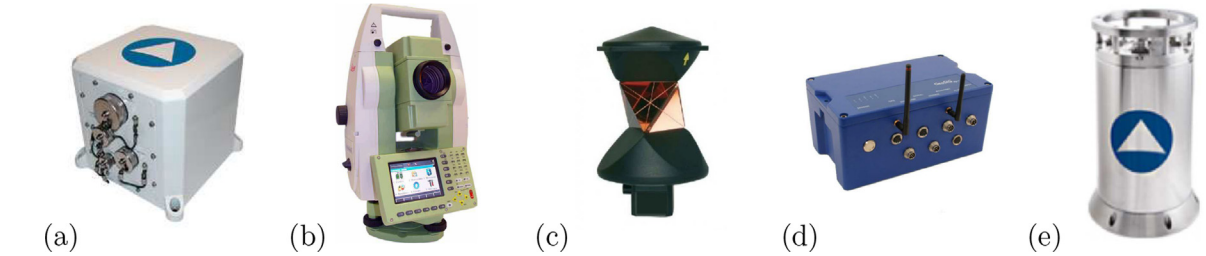


**Fig. 3.** Overview of the measurement equipment: (a) the iXBlue HYDRINS Inertial Navigation System, (b) a Leica TCRP 1201 total station, (c) a Leica 360 YR20A prism, (d) a GeoSIG wireless GMS-18 recorder, and (e) the iXBlue OCTANS 3000 subsea high performance Attitude Heading Reference System.

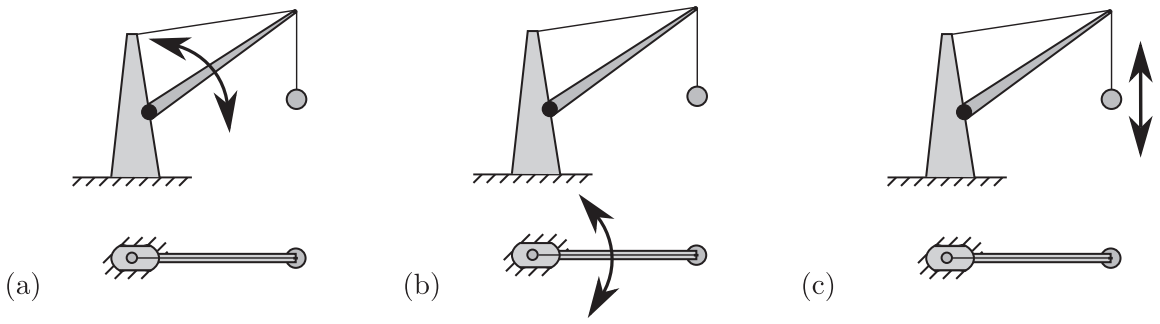


**Fig. 5.** Schematic representation of (a) a luffing operation, (b) a slewing operation, and (c) a hoisting operation (top: side view crane, bottom: top view crane).

sampling rate of 200 Hz has been used in the A/D conversion. The acceleration measurements have an accuracy of $\pm$ 1.2 $\times$ $10^{-4}$ m/s$^2$. The GeoSIG GMS-18 recorders use an intelligent Real Time Clock (RTC) with a self-learning temperature compensation. The RTC of each recorder is synchronized with GPS. The GMS-18 units are installed inside the turbine blade. Each of the units has been installed in a steel cabinet to protect the sensor from the environment and to secure power supply and network connection. The cabinets are wedged to the structure of the blade.

### 2.2. Crane boom and Boom Lock©

The measurements on the crane boom and the Boom Lock© have been performed using four wireless GeoSIG GMS-18 recorders and an iXBlue OCTANS 3000 subsea high performance Attitude Heading Reference System. Fig. 6 gives an overview of the measurement locations.

*GeoSIG GMS-18.* The same GeoSIG GMS-18 acceleration recorders as installed on the blade (Section 2.1) have been installed in a steel cabinet on the crane boom and Boom Lock© (see Fig. 6). Three GMS-18 recorders have been installed on the crane boom (`P1`, `B1`, and `B2`) and one recorder has been installed on the Boom Lock© (`BL1`).

*iXBlue OCTANS 3000.* An iXBlue OCTANS 3000 subsea high performance Attitude Heading Reference System has been installed on the crane boom to monitor the topping and slewing operations of the crane (see Fig. 5). The OCTANS 3000 includes three fiber optic gyroscope (FOG) sensors and a three-axial accelerometer to measure its three-dimensional motion (3 translations, 3 rotations). The OCTANS 3000 performs a real-time processing of the acceleration and gyroscope data, hereby obtaining the motion of the sensor (3 translations, 3 rotations) at a sampling rate of 25 Hz. The translations are purely based on the integration of acceleration data. Due to measurement noise, the low frequency translations cannot be retrieved from the acceleration data. Only the rotations obtained from the OCTANS 3000 have been used in the analysis. The data obtained from the OCTANS 3000 received a timestamp from the GPS (Section 2.1) that was sent through a WiFi network.

The analysis presented in the following is based on the blade motion relative to the motion induced by the crane operations (slewing, luffing, and lifting operations, see Fig. 5). An additional logging system has therefore been used to collect information on the hoist configuration (luffing and slewing angle of the crane boom, position of the Boom Lock© along the crane boom, etc.). This information is essential in the processing and interpretation of the data. The logging system was also used to collect the wind speed and direction. A sampling rate of 1 sample per second (i.e. 1 Hz) is used. The logging data are synchronized manually with the GPS-timestamped data obtained from the other sensors (HYDRINS, OCTANS 3000 and GMS-18 units), by matching the slewing angle obtained from the logging system and the crane heading obtained from the OCTANS 3000 installed on the crane boom.

## 3. Blade motion analysis

### 3.1. Data processing

The motion of the turbine blade is calculated for two reference points on the blade, i.e. the blade root (see Fig. 2, $x = -17.93$ m, $y = 0$ m, $z = 0$ m) and the COG ($x = 0$ m, $y = 0$ m, $z = 0$ m). The translations of the reference points consist of (1) the longitudinal displacement $u$, defined along the $x$-axis, (2) the lateral displacement $v$, defined along the $y$-axis, and (3) the vertical displacement $w$, defined along the $z$-axis. The rotations of the turbine blade (heading $\psi$, pitch $\theta$, and roll $\phi$) are defined in Fig. 7. The heading is defined positive clockwise around the $z$-axis, the pitch is defined positive counterclockwise around the $y'$-axis, and the roll is defined positive counterclockwise around the $x''$-axis. The translations and rotations are calculated (1) from the RTK-GPS/INS data and (2) from the Leica data, as outlined next.

*Processing data RTK-GPS/INS.* The (post-processed) RTK-GPS/INS data are first re-sampled at 5 Hz by applying linear interpolation between the consecutive data points, hereafter applying elementary coordinate transformations to calculate the motion of the two reference points on the blade (3 translations, 3 rotations). When assuming rigid body motion of the blade, the rotations do not depend on the particular point considered. The rotations of the blade for a time $t$ are directly obtained from the measured rotations ($\psi_H$, $\theta_H$, and $\phi_H$) obtained from

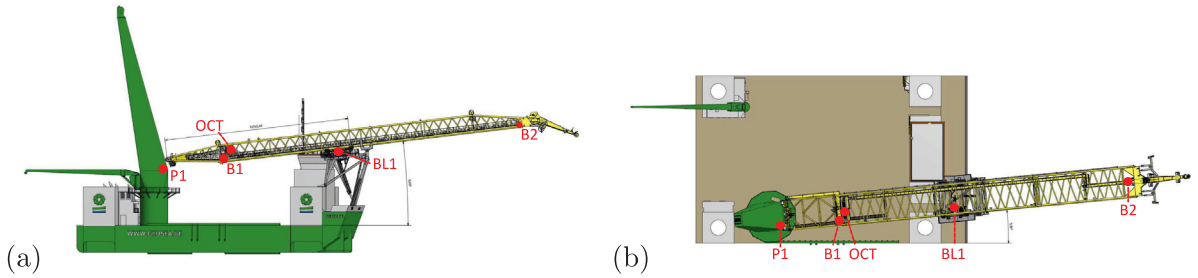


**Fig. 6.** (a) Side view and (b) top view of the jack up vessel Neptune and the mast crane indicating the sensor positions (`OCT`: OCTANS, `Pi`: GeoSIG GMS-18 unit *i* at the crane pivot, `Bi`: GeoSIG GMS-18 unit *i* at the crane boom, and `BLi`: GeoSIG GMS-18 unit *i* at the Boom Lock©).

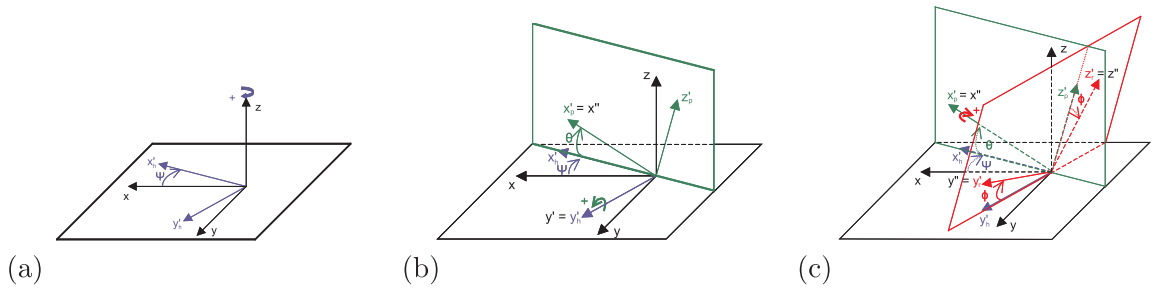


**Fig. 7.** Definition of (a) heading motion, (b) pitch motion, and (c) roll motion, according to [18].

the HYDRINS system:

$$\psi(t) = \psi_{\mathrm{H}}(t), \quad \theta(t) = \theta_{\mathrm{H}}(t), \quad \phi(t) = \phi_{\mathrm{H}}(t) \tag{1}$$

Calculation of the translations requires additional processing of the data. Under the assumption of rigid body motion, the translations of a point on the blade with coordinates $x, y$, and $z$, are calculated as [18]:

$$\begin{bmatrix} u(x,y,z,t) \\ v(x,y,z,t) \\ w(x,y,z,t) \end{bmatrix} = \begin{bmatrix} u_{\mathrm{H}}(t) \\ v_{\mathrm{H}}(t) \\ w_{\mathrm{H}}(t) \end{bmatrix} + \mathbf{T}_{\psi}(t)\mathbf{T}_{\theta}(t)\mathbf{T}_{\phi}(t) \begin{bmatrix} x-x_{\mathrm{H}} \\ y-y_{\mathrm{H}} \\ z-z_{\mathrm{H}} \end{bmatrix} \tag{2}$$

where $u_{\mathrm{H}}, v_{\mathrm{H}}$, and $w_{\mathrm{H}}$ denote the translations obtained from the HYDRINS system, $x_{\mathrm{H}}, y_{\mathrm{H}}$, and $z_{\mathrm{H}}$ the coordinates of the HYDRINS system, and $\mathbf{T}_{\psi}$, $\mathbf{T}_{\theta}$, and $\mathbf{T}_{\phi}$ the transformation matrices corresponding to heading, pitch, and roll motion, respectively, defined by:

$$\begin{aligned} \mathbf{T}_{\psi} &= \begin{bmatrix} \cos\psi & \sin\psi & 0 \\ -\sin\psi & \cos\psi & 0 \\ 0 & 0 & 1 \end{bmatrix}, \\ \mathbf{T}_{\theta} &= \begin{bmatrix} \cos\theta & 0 & \sin\theta \\ 0 & 1 & 0 \\ -\sin\theta & 0 & \cos\theta \end{bmatrix}, \\ \mathbf{T}_{\phi} &= \begin{bmatrix} 1 & 0 & 1 \\ 0 & \cos\phi & -\sin\phi \\ 0 & \sin\phi & \cos\phi \end{bmatrix} \end{aligned} \tag{3}$$

*Processing data Leica total stations.* The data obtained from the three Leica total stations are first interpolated to a common time base, using a sampling rate of 5 Hz. The re-sampled Leica data are subsequently used to calculate the motion of the two reference points, hereby assuming rigid body motion of the blade. As a first step in this process, one has to determine the rotational matrix $\mathbf{T} \in \mathbb{R}^{3\times3}$ that defines the rotation between the original coordinate system *xyz* and the actual coordinate system *x"y"z"* that follows the imposed blade motion for every time step *t*. The problem of seeking a rotational matrix between two coordinate systems based on a set of vector observations was first posed by G. Wahba and is therefore in the literature known as Wahba's problem [21].

In accordance to [21], the transformation matrix $\mathbf{T}$ is determined for every time step $t$ by minimization of the following cost function $J$:

$$J(\mathbf{T}(t)) = \frac{1}{2}\sum_{k=2}^{3} \alpha_k \left\| \begin{bmatrix} u_{\mathrm{Prk}}(t)-u_{\mathrm{Pr1}}(t) \\ v_{\mathrm{Prk}}(t)-v_{\mathrm{Pr1}}(t) \\ w_{\mathrm{Prk}}(t)-w_{\mathrm{Pr1}}(t) \end{bmatrix} - \mathbf{T}(t) \begin{bmatrix} x_{\mathrm{Prk}}-x_{\mathrm{Pr1}} \\ y_{\mathrm{Prk}}-y_{\mathrm{Pr1}} \\ z_{\mathrm{Prk}}-z_{\mathrm{Pr1}} \end{bmatrix} \right\|_2^2 \tag{4}$$

where $u_{\mathrm{Pr}\,k}, v_{\mathrm{Pr}\,k}, w_{\mathrm{Pr}\,k}$, and $x_{\mathrm{Pr}\,k}$, $y_{\mathrm{Pr}\,k}$, $z_{\mathrm{Pr}\,k}$, denote the measured translations and the reference coordinates of a prism $k$, respectively, and $\alpha_k$ are optional weighting factors. Since the three Leica total stations have the same measurement accuracy, the weighting factors $\alpha_k$ are all assumed to be 1 in this case.

The solution of Wahba's problem implemented here is the one provided by Markley in [22]. The transformation matrix $\mathbf{T}$ that minimizes the least squares cost function in Eq. (4) is calculated as follows:

$$\mathbf{T} = \mathbf{U}\mathbf{M}\mathbf{V}^{\mathrm{T}} \tag{5}$$

where $\mathbf{U} \in \mathbb{R}^{3\times3}$ and $\mathbf{V} \in \mathbb{R}^{3\times3}$ are the left respectively right singular vectors obtained from the following singular value decomposition (SVD):

$$\mathbf{U}\mathbf{S}\mathbf{V}^{\mathrm{T}} = \sum_{k=2}^{3} \left( \begin{bmatrix} u_{\mathrm{Prk}}-u_{\mathrm{Pr1}} \\ v_{\mathrm{Prk}}-v_{\mathrm{Pr1}} \\ w_{\mathrm{Prk}}-w_{\mathrm{Pr1}} \end{bmatrix} \begin{bmatrix} x_{\mathrm{Prk}}-x_{\mathrm{Pr1}} \\ y_{\mathrm{Prk}}-y_{\mathrm{Pr1}} \\ z_{\mathrm{Prk}}-z_{\mathrm{Pr1}} \end{bmatrix}^{\mathrm{T}} \right) \tag{6}$$

The matrix $\mathbf{M}$ in Eq. (5) is calculated as

$$\mathbf{M} = \mathrm{diag}(1,\ 1,\ \det(\mathbf{U})\det(\mathbf{V})) \tag{7}$$

As shown in [22], the SVD provides a robust procedure for the determination of the transformation matrix. The reader is referred to [22] for more information on the algorithm.

Once the transformation matrix $\mathbf{T}$ has been determined, the translations of a point on the blade with coordinates $x, y$, and $z$, are calculated as:

$$\begin{bmatrix} u(x,y,z,t) \\ v(x,y,z,t) \\ w(x,y,z,t) \end{bmatrix} = \begin{bmatrix} u_{\mathrm{Pr1}}(t) \\ v_{\mathrm{Pr1}}(t) \\ w_{\mathrm{Pr1}}(t) \end{bmatrix} + \mathbf{T}(t) \begin{bmatrix} x-x_{\mathrm{Pr1}} \\ y-y_{\mathrm{Pr1}} \\ z-z_{\mathrm{Pr1}} \end{bmatrix} \tag{8}$$

The rotations of the blade are obtained from the transformation matrix $\mathbf{T}$ as follows:

$$\psi(t) = -\mathrm{sign}(\mathbf{T}_{[2,1]}(t))\arccos\left( \frac{\mathbf{T}_{[1,1]}(t)}{\sqrt{\mathbf{T}^2_{[1,1]}(t) + \mathbf{T}^2_{[2,1]}(t)}} \right) \tag{9}$$

$$\theta(t) = -\mathrm{sign}(\mathbf{T}_{[3,1]}(t)) \arccos\left( \frac{\sqrt{\mathbf{T}^2_{[1,1]}(t) + \mathbf{T}^2_{[2,1]}(t)}}{\sqrt{\mathbf{T}^2_{[1,1]}(t) + \mathbf{T}^2_{[2,1]}(t) + \mathbf{T}^2_{[3,1]}(t)}} \right) \tag{10}$$

$$\phi(t) = \mathrm{sign}(\mathbf{T}_{[3,2]}(t)) \arccos\left( \frac{\mathbf{T}_{[1,2]}(t)\sin(\psi(t)) + \mathbf{T}_{[2,2]}(t)\cos(\psi(t))}{\sqrt{\mathbf{T}^2_{[1,2]}(t) + \mathbf{T}^2_{[2,2]}(t) + \mathbf{T}^2_{[3,2]}(t)}} \right) \tag{11}$$

where $\mathbf{T}_{[k,l]}$ denotes the element on the $k$-th row and the $l$-th column of the rotation matrix $\mathbf{T}$ and $\mathrm{sign}(\alpha)$ returns 1 if $\alpha \geq 0$ and $-1$ if $\alpha < 0$.

Uncertainty on the translations and rotations obtained from Eqs. (8)–(11) is due to three different types of errors. First, errors in the reference coordinates of the prisms $x_{\mathrm{Pr}\,k}, y_{\mathrm{Pr}\,k}$, and $z_{\mathrm{Pr}\,k}$ lead to a bias in the estimation. Second, so-called measurement noise leads to small errors on the measured translations $u_{\mathrm{Pr}\,k}$,$v_{\mathrm{Pr}\,k}$, and $w_{\mathrm{Pr}\,k}$, which lead in turn to stochastic errors on the estimated translations and rotations. Third, vibrations of the blade in addition to its rigid body motion lead to a violation of the underlying assumptions of Wahba's problem, where only rigid body motion is considered. In the considered case, it can be expected that the errors in the reference coordinates constitute the most important source of uncertainty. Indeed, it was found that the distance between the three prisms changes by 5 to 10 cm when lifting the blade, due to bending of the blade under its own weight. This inevitably introduces an error in the reference coordinates $x_{\mathrm{Pr}\,k}, y_{\mathrm{Pr}\,k}$, and $z_{\mathrm{Pr}\,k}$. Although these errors are not directly accounted for in the estimation, one should keep the different possible sources of uncertainty in mind when

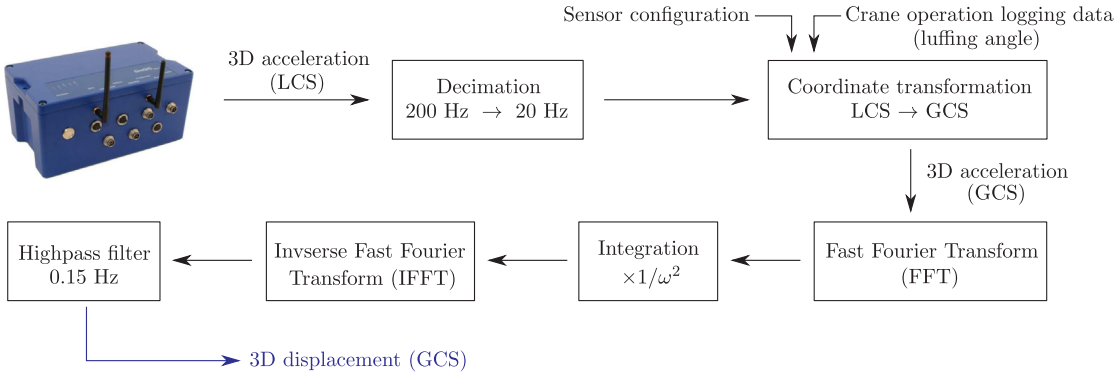


**Fig. 8.** Schematic representation the acceleration data processing.

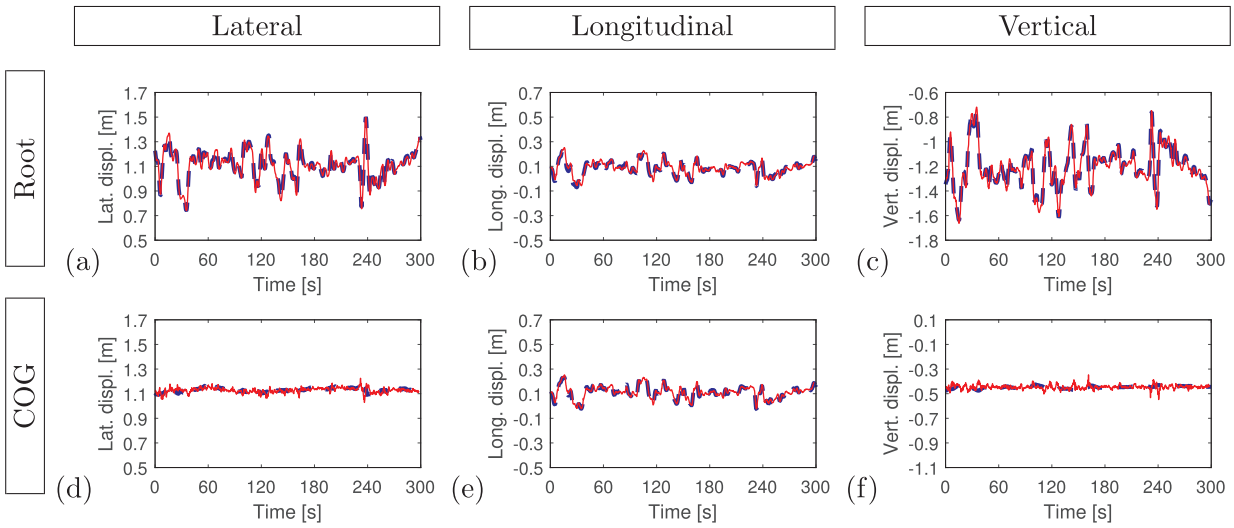


**Fig. 9.** Time history of the lateral displacement (left), longitudinal displacement (middle) and vertical displacement (right) of the blade root ((a)–(c)) and the blade COG ((d)–(f)). The blue dashed line shows the motion obtained from the RTK-GPS/INS measurement system, the red solid line the motion obtained from the Leica measurement system. (For interpretation of the references to color in this figure legend, the reader is referred to the web version of this article.)

interpreting the results.

In order to obtain the motion of the blade relative to the motion induced by the crane operations (slewing, luffing, and lifting, see Fig. 5), the motion that is directly induced by the crane operations is subtracted from the blade motion obtained from both the RTK-GPS/INS data and the Leica data. The logging data (i.e. slewing angle, luffing angle, and paid out length of the main hoist) are used in the transformation of the motion data.

The displacements of the crane boom and Boom Lock© relative to the static deflection under deadweight are obtained by double integration of the measured accelerations. Fig. 8 provides a scheme of the acceleration data processing. The accelerations measured in a sensor-specific local coordinate system (LCS) are first decimated. The decimation consist of applying an eighth-order Chebychev type I digital lowpass filter with a cutoff frequency of 8 Hz, both in the forward and the reverse direction to remove all phase distortion, and then re-sampling the data at 20 Hz. All acceleration data are subsequently transformed into the right handed global coordinate system (GCS) *xyz* of the turbine blade (see Fig. 2). In the transition of coordinate systems, it is assumed that the axis of the blade (i.e. the *y*-axis) is situated in the horizontal plane and is perpendicular to the axis of the crane boom, with the COG of the blade (i.e. the origin of the coordinate system *xyz*) located right below the top of the mast crane. The three acceleration signals obtained for each sensor in this way correspond to (1) the lateral direction, (2) the longitudinal direction of the turbine blade in its fixed reference configuration, and (3) the vertical direction. The resulting acceleration signals are integrated twice to obtain displacement signals. The integration is performed in the frequency domain, dividing the Fourier transform of the displacement by $\omega^2$, where $\omega$ is the angular frequency in rad/s. The displacement signals obtained are passed through a fifth order Chebyshev type I high-pass filter with a cutoff frequency of 0.15 Hz and a filter ripple in the passband of 0.01 dB. The aim of the filter is to remove the low frequency components from the signals which are contaminated by measurement noise on the acceleration data.

### 3.2. Results

Figs. 9 and 10 compare time history of the motion of the blade after lifting (translations and rotations, respectively) obtained from (1) the RTK-GPS/INS measurement system, and (2) the Leica measurement system, for a time range of 5 min. Figs. 11 and 12 show the time history of the difference in motion obtained from the two measurement systems, hereby also indicating the RMS difference values.

It is observed that the blade motion obtained from both measurement systems in Figs. 9 and 10 describes the same overall behavior, where the blade motion is mainly a combination of longitudinal motion and heading and pitch motion around the blade COG. The longitudinal motion of the blade root and its COG are nearly identical. This is expected, since both points are rigidly connected. Meanwhile, the heading and pitch motion around the blade COG lead in turn to a significant lateral and vertical motion at the blade root, whereas the lateral and

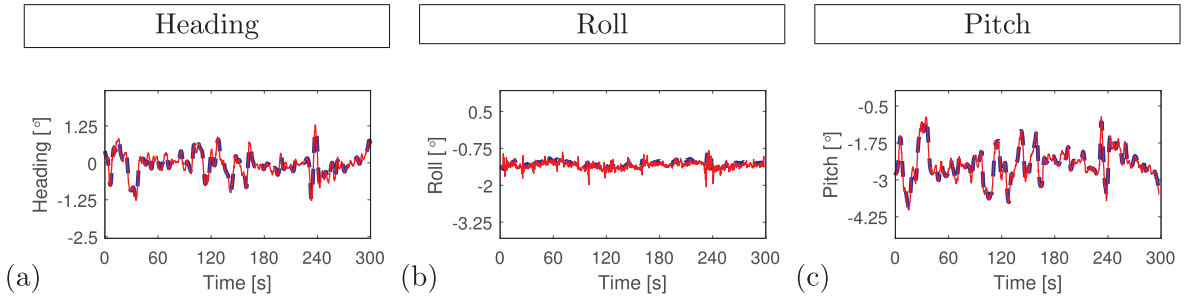


**Fig. 10.** Time history of (a) the heading, (b) the pitch, and (c) the roll of the blade. The blue dashed line shows the motion obtained from the RTK-GPS/INS measurement system, the red solid line the motion obtained from the Leica measurement system. (For interpretation of the references to color in this figure legend, the reader is referred to the web version of this article.)

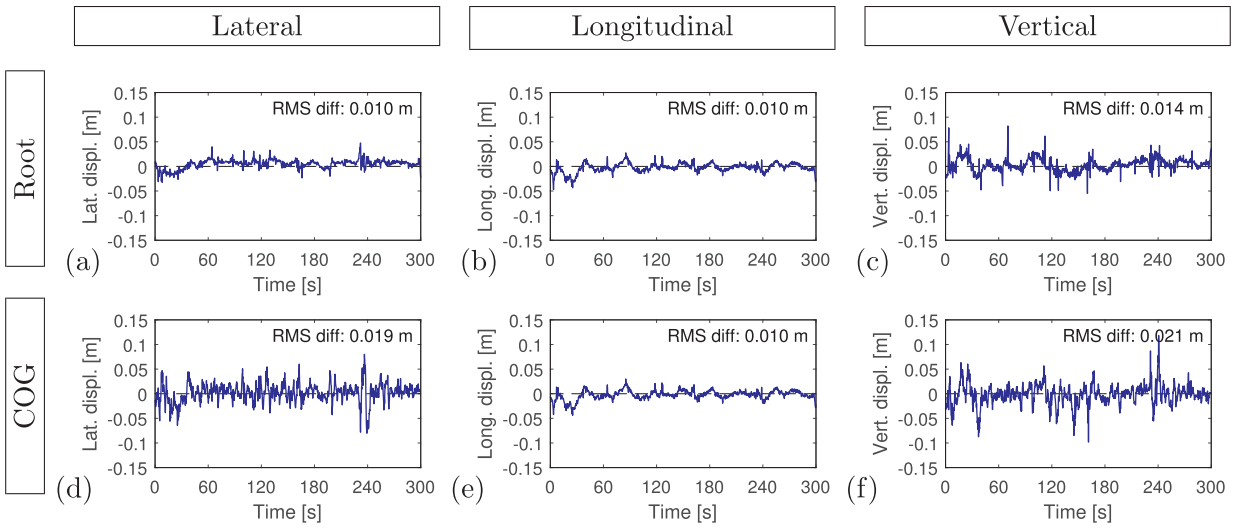


**Fig. 11.** Time history of the difference in lateral displacement (left), longitudinal displacement (middle) and vertical displacement (right) of the blade root ((a)–(c)) and the blade COG ((d)–(f)).

vertical motion of the blade COG are very small. Notice the very large correlation between the heading motion and the lateral motion of the blade root and similarly between the pitch motion and the vertical motion of the blade root.

Overall, a very good agreement is obtained between the motion obtained from both measurement systems. Focusing on the differences in the blade motion in Figs. 11 and 12, it is firstly found that the observed differences for both the translations and the rotations are all of the same order of magnitude. This also follows from a comparison of the RMS difference values, which range from 0.010 m to 0.021 m for the translations and 0.070° to 0.115° for the rotations. Note that the differences are intentionally not referred to as errors, since the motion obtained from both systems is characterized by estimation errors, whereas the actual blade motion is unknown. The observed differences are mainly attributed to measurement noise and the static deformation of the blade under its own weight, which leads to significant errors in the so-called sensor reference coordinates that are assumed in the data processing (see also Section 3.1). Note that the processing of the Leica data relies on the reference locations of the three prisms, whereas the RTK-GPS/INS system measures the motion of the blade root directly (translations and rotations). The motion of the RTK-GPS/INS system is only sensitive to errors in the measurement setup when it comes to the extrapolation of the motion to the blade COG.

Fig. 13 shows the displacements at the boom tip (sensor `B2`, Fig. 6) for the same time interval considered Figs. 9 and 10. The displacements have been obtained by integration of the measured accelerations, as described in Section 3.1. Comparison of the (dynamic) displacements of the boom to the displacements of the blade allows to investigate

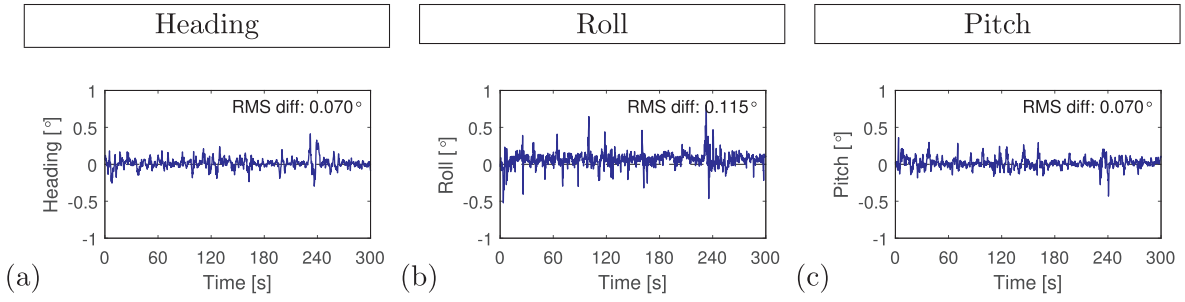


**Fig. 12.** Time history of the difference in (a) the heading, (b) the pitch, and (c) the roll of the blade.

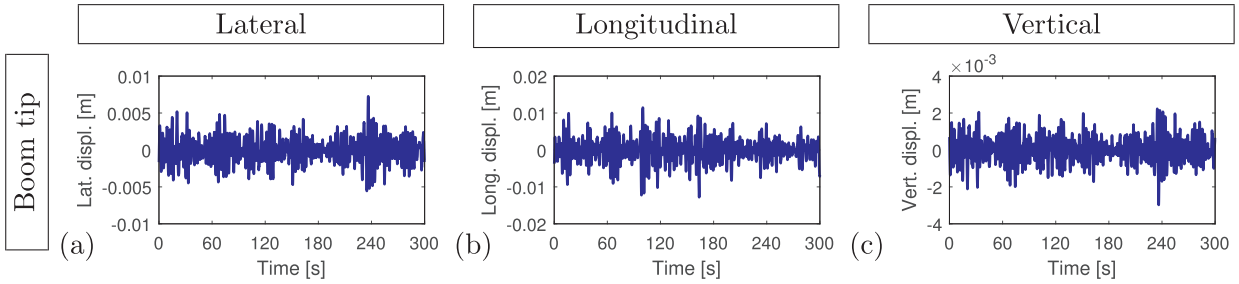


**Fig. 13.** Time history of (a) the lateral displacement, (b) the longitudinal displacement, and (c) the vertical displacement of the boom tip (sensor B2).

whether the motion of the blade is mainly imposed by the crane (cfr. base motion) or whether it is caused by the wind loads which lead to a relative motion of the blade with respect to the crane. For the lateral and longitudinal motion, the displacement levels at the boom tip are much smaller than the displacement levels (translations) obtained at the COG of the blade. The lateral and longitudinal motion of the blade mainly consists of quasi-static motion at frequencies much lower than the natural frequencies of the crane boom. The vertical displacement levels at the boom tip are slightly smaller than those observed at the COG of the blade. In this case, it can be assumed, however, that the vertical motion at the boom tip is nearly identical to the vertical motion at the blade COG, due to the high axial stiffness of the cable connecting the boom tip to the blade gripper. This is not observed from the measurements. The observed difference stems from (inevitable) highpass filtering of the displacements at the boom tip after the integration, hereby removing the low frequency motion.

## 4. Conclusions

This paper presents an application of an RTK-GPS/INS measurement system for motion tracking of a 6 MW wind turbine blade during lifting. It is found that the RTK-GPS/INS measurement system allows for very accurate recording of displacement and rotation and as such provides essential information to reveal the (rigid body) motion of a system. This in combination with the fact that it does not require a fixed reference point in the direct environment of the structure makes RTK-GPS/INS particularly suited for motion tracking on offshore and other large civil engineering structures. Although the blade motion is only shown for a measurement period of 300 s, the results were found to be very repeatable.

## Acknowledgements

The presented research has been performed within the framework of the project G.0738.11 “Inverse identification of wind loads on structures”, funded by the Research Foundation Flanders (FWO), Belgium. Kristof Maes is a postdoctoral fellow of FWO. The financial support of FWO and KU Leuven is gratefully acknowledged. The experiments have been organized by High Wind NV and carried out by KU Leuven. The authors would like to thank High Wind NV for allowing the publication of the data. The authors also thank GeoSea NV for their contribution to the experiments.

## References

[1] Nassif H, Gindy M, Davis J. Comparison of laser Doppler vibrometer with contact sensors for monitoring bridge deflection and vibration. NDT&E Int 2005;38:213–8.
[2] Maes K, Van Nimmen K, Lourens E, Rezayat A, Guillaume P, De Roeck G, et al. Verification of joint input-state estimation for force identification by means of in situ measurements on a footbridge. Mech Syst Signal Process 2016;75:245–60.
[3] Stanbridge A, Ewins D. Modal testing using a scanning laser Doppler vibrometer. Mech Syst Signal Process 1999;13:255–70.
[4] Siringoringo D, Fujino Y. Experimental study of laser Doppler vibrometer and ambient vibration for vibration-based damage detection. Eng Struct 2006;28:1803–15.
[5] Yang S, Allen M. Output-only modal analysis using continuous-scan laser Doppler vibrometry and application to a 20 kW wind turbine. Mech Syst Signal Process 2012;31:228–45.
[6] Lee J, Shinozuka M. Real-time displacement measurement of a flexible bridge using digital image processing techniques. Exp Mech 2006;46:105–14.
[7] Lee J, Shinozuka M. A vision-based system for remote sensing of bridge displacement. NDT&E Int 2006;39:425–31.
[8] Fujino Y, Murata M, Okano S, Takeguchi M. Monitoring system of the Akashi Kaikyo bridge and displacement measurement using GPS. Proceedings of SPIE, vol. 3995. 2000. p. 229–36.
[9] Van Le H, Nishio M. Time-series analysis of GPS monitoring data from a long-span bridge considering the global deformation due to air temperature changes. J Civ Struct Health Monit 2015;5:415–25.
[10] Wang H, Guo T, Tianyou T. Establishment and application of the wind and structural health monitoring system for the Runyang Yangtze River bridge. Shock Vib 2014.
[11] Xu L, Guo J, Jiang J. Time-frequency analysis of a suspension bridge based on GPS. J Sound Vib 2002;254:105–16.
[12] Meo M, Zumpano G, Meng X, Cosser E, Roberts G, Dodson A. Measurements of dynamic properties of a medium span suspension bridge by using the wavelet transforms. Mech Syst Signal Process 2006;20:1112–33.
[13] Park K-T, Kim S-H, Park H-S, Lee K-W. The determination of bridge displacement using measured acceleration. Eng Struct 2005;27:371–8.
[14] Gross J, Gu Y, Rhudy M, Gururajan S, Napolitano M. Flight-test evaluation of sensor fusion algorithms for attitude estimation. IEEE Trans Aerosp Electron Syst 2012;48:2128–39.
[15] Petovello M, Cannon M, Lachapelle G, Wang J, Wilson C, Salychev O, et al. Development and testing of a real-time GPS/INS reference system for autonomous automobile navigation. Proceedings of the 14th international technical meeting of the satellite division of the institute of navigation. Salt Lake City, Utah, USA: ION GPS; 2001. p. 229–36.
[16] El-Sheimy N, Eun-Hwan S, Xiaoji N. Kalman filter face-off: extended vs. unscented Kalman filters for integrated GPS and MEMS inertial. Inside GNSS 2006:48–54.
[17] DELPH INS bv. 2.4, user guide, iXBlue, 2013.
[18] Inertial Products, Principle & Conventions, iXBlue, 2014.
[19] Julier S, Uhlmann J, Durrant-Whyte H. A new method for the nonlinear transformation of means and covariances in filters and estimators. IEEE Trans Autom Control 2000;45:477–82.
[20] Wan E, van der Merwe R. The unscented Kalman filter for nonlinear estimation. Proceedings of the IEEE 2000 adaptive systems for signal processing, communications, and control symposium, Lake Louise, Alberta, Canada. 2000. p. 153–8.
[21] Wahba G. Problem 65-1: a least squares estimate of spacecraft attitude. SIAM Rev 1965;7:409.
[22] Markley F. Attitude determination using vector observations and the singular value decomposition. J Astronaut Sci 1988;38:245–58.